

# European ECOSTRESS Hub 2

## ATBD Daily ET

Reference: D1.1-ATBD-DailyET

ESA Contract No. 4000129873/20/I-NS

Prepared by	Tian Hu, Kaniska Mallick, Patrik Hitzelberger and Yoanne Didry (LIST)
Reference	D1.1-ATBD-DailyET
Issue	1
Revision	2
Date of Issue	2025-01-14
Status	<b>Initial Version</b>
Document Type	Algorithm Theoretical Basis Document Daily Evapotranspiration
Distribution	LIST, ESA

## DISTRIBUTION LIST

<b>Name</b>	<b>Affiliation</b>
Zoltan Szantoi	ESA
Tian Hu	LIST
Kaniska Mallick	LIST
Patrik Hitzelberger	LIST
Yoanne Didry	LIST

## APPROVAL

<b>Name</b>	<b>Affiliation</b>	<b>Date</b>	<b>Signature</b>
Zoltan Szantoi	ESA		

## CHANGE LOG

<b>Issue</b>	<b>Revision</b>	<b>Date</b>	<b>Author</b>	<b>Comment</b>
1	0	2025-01-02	Hu, Mallick, Lin, Hitzelberger, Didry	Initial version
1	1	2025-01-10	Hu, Mallick, Lin, Hitzelberger, Didry	Initial version edited and commented by KM (sent to ESA)
2	0	2025-01-14	Hu, Mallick, Lin, Hitzelberger, Didry	Updated version with comments from ESA

## List of abbreviation

<b>Abbreviation</b>	<b>Full name</b>
CGLS	Copernicus Global Land Surface
EEH2	European ECOSTRESS Hub Phase 2
EF	Evaporative fraction
EFDC	European Fluxes Database Cluster
ET	Evapotranspiration
ICOS	Integrated Carbon Observations System
LST	Land surface temperature
LUT	Look up table
PM	Penman-Monteith
SEB	Surface energy balance
STIC	Surface Temperature Initiated Closure
SEBS	Surface Energy Balance System
TSEB	Two-Source Energy Balance

# Contents

<b>Abstract</b> .....	6
<b>1. Introduction</b> .....	8
<b>2. Theory and basis</b> .....	10
2.1. Instantaneous ET estimation .....	10
2.2. Commonly used approaches for temporal upscaling of instantaneous ET .....	11
<b>3. Look up table-based extraterrestrial radiation method</b> .....	14
3.1. Selection of the constraining factors .....	15
3.2. Calibration of the LUT .....	16
3.3. Evaluation of the LUT-based extraterrestrial radiation method.....	19
<b>Acknowledgement</b> .....	25
<b>Reference</b> .....	26

## Abstract

Daily evapotranspiration (ET) is an important variable in global hydrological cycle investigation, climate change studies, and agricultural water resource management. While a spectrum of research disciplines relies on remote sensing based daily ET ( $ET_d$  hereafter) estimates, the remotely-sensed ET retrievals are usually done for a single snapshot at the time of satellite overpass of the polar orbiting sensors. The estimated instantaneous ET does not satisfy the expectations of hydrologists, irrigation engineers, or water resource managers in practical applications (Tang et al., 2013). Therefore, temporal integration is required to convert the instantaneous ET to the daily scale (Wandera et al., 2017).

Different models have been developed with regard to the daily upscaling of ET. These models can be categorized as either evaporative fraction-based or radiation-based. One of most commonly used approaches is the constant evaporative fraction (EF) method. In this approach, the ratio of latent heat flux to surface available energy (surface net radiation minus soil heat flux) is assumed to be conserved. In addition, the reference evaporative fraction ( $EF_r$ ) method is also commonly adopted in  $ET_d$  estimation. This method assumes that the ratios of actual to reference grass/alfalfa ET at different time scales are constant. Another widely used approach is based on the conservation of the ratio of ET to surface solar radiation ( $R_g$ ) considering the solar radiation is the primary energy driver of surface water and energy transfer at the land surface. To avoid the calculation of daily solar radiation, the extraterrestrial solar radiation ( $R_p$ ) method is also developed by substituting the surface solar radiation with the top-of-atmosphere solar radiation.

Although the aforementioned methods have been successfully applied to estimate daily ET for different operational polar orbiting satellites, the asynchronous orbit of ECOSTRESS challenges the usability of these approaches considering the varying overpass times. Furthermore, the theoretical assumption of the conservation of EF and  $EF_r$  and symmetrical response of ET to  $R_g$  and  $R_p$  during the course of the day may not hold across

climates and aridity. Therefore, an innovative method considering the various constraining factors at different times of the day and in different ecosystems is in an urgent need to generate  $ET_d$  information from ECOSTRESS.

**In the European ECOSTRESS Hub Phase 2 (EEH2), a new temporal integration method for instantaneous to daily ET has been developed to accommodate the varying overpass times of ECOSTRESS.** The method employs a lookup table (LUT) constructed based on satellite overpass times and ecosystem types. This ATBD provides a detailed explanation of the LUT-based approach for daily ET estimation.

## 1. Introduction

Evapotranspiration (ET) is a critical component in the terrestrial water cycle, and it quantifies the amount of water loss from the Earth's surface to atmosphere (Jasechko et al., 2013). By dissipating net available energy through latent heat flux, ET cools down the land surface. As with global warming and drying over many land areas (Dai, 2013), ET mapping becomes increasingly important to understand the impacts of global change on terrestrial biosphere for developing adaptive strategies. ET estimates from satellite observations are snapshots at the satellite overpass times. However, instantaneous ET cannot be used without much practical significance to most applications, stressing the need for daily (or even longer period) integration.

The key to the development of various ET upscaling method is to relate the targeted longer time-scale ET to a factor that can be assumed to be constant during the daytime or throughout a diurnal cycle (Tang et al., 2013). Four methods are commonly used, including the evaporative fraction (EF) method (Galleguillos et al., 2010), the reference evaporative fraction ( $EF_r$ ) method (Allen et al., 2007), the surface solar radiation ( $R_g$ ) method (Wandera et al., 2017), and the extraterrestrial solar radiation ( $R_p$ ) method (Ryu et al., 2012). All these methods are developed based on the assumption that the ratios of ET to the scaling factor (e.g., net available energy, reference evapotranspiration, surface solar radiation, or extraterrestrial solar radiation) at the instantaneous and daily time scales stay the same. However, the assumed conservation can be jeopardized by various factors. Moreover, these methods fail to account for the temporal changes in atmospheric conditions that can have significant influence on daily ET retrieval.

Based on the aforementioned methods of daily ET estimation, a look-up-table (LUT) based method is proposed to upscale the instantaneous ET using the extraterrestrial solar radiation. In this new approach, the environmental conditions will be incorporated into the traditional  $R_p$  method across climates and ecosystems. In this way, the advantages of the

aforementioned methods will be combined in a simple and straightforward manner. Moreover, the varying overpass times of ECOSTRESS due to its asynchronous orbit is explicitly accounted for. This ATBD will elaborate on the development of this new ET temporal integration method.

## 2. Theory and basis

ET is intrinsically associated with the surface energy balance (SEB, hereafter) equation, depending on the partitioning of net available energy into sensible and latent heat fluxes. The SEB equation is written as follows:

$$R_N = \lambda E + H + G \quad (2.1)$$

where  $H$  and  $\lambda E$  are sensible and latent heat fluxes ( $W\ m^{-2}$ ), respectively,  $G$  is the ground heat conduction flux. The segregation of net available energy (the difference between net radiation  $R_N$  and ground heat flux  $G$ ) in these two different convective fluxes depends on the land surface moisture status, atmospheric conditions in the boundary layer, and biophysical control of vegetation. The estimated ET using the satellite observations based on the SEB model indicates the instantaneous energy flux at the satellite overpass time. A temporal upscaling model is required to integrate the instantaneous ET during the course of the day for estimating the daily ET.

### 2.1. Instantaneous ET estimation

In the EEH Phase 1 (EEH1), three structurally different SEB models were implemented on the ECOSTRESS data for the ET product development, including the analytical Surface Temperature Initiated Closure (STIC) model, the one-source parametric Surface Energy Balance System (SEBS) model, and the Two-Source Energy Balance (TSEB) parametric model.

A comprehensive evaluation of the EEH instantaneous ET products was conducted with respect to flux measurements from 19 eddy covariance sites in Europe over 6 different ecosystems with diverse aridity levels (Hu et al., 2023). It was revealed that the STIC model had a comparable performance to the SEBS model (with an overall RMSE of  $\sim 70\ W\ m^{-2}$ ). Nevertheless, the relatively complex TSEB model produced a high RMSE of  $\sim 90\ W\ m^{-2}$ . Comparison between STIC ET estimates and the operational ECOSTRESS ET product from NASA PT-JPL model showed a larger RMSE (around  $50\ W\ m^{-2}$  higher) for the PT-JPL ET

estimates. Substantial overestimation ( $>80 \text{ W m}^{-2}$ ) in PT-JPL ET estimates was evident over shrublands and savannas, presumably due to weak constraint of land surface temperature (LST) in the model. Considering the good accuracy of STIC relative to the other SEB models, only the STIC model is planned to be adopted in the EEH 2 for the retrieval of the instantaneous ET and developing  $\text{ET}_d$  data product. A brief introduction of the STIC model is given as follows.

The one-source STIC model was first proposed by Mallick et al. (2014). STIC is based on the integration of radiometric temperature into the Penman-Monteith (PM) formulation to find the analytical solution of the aerodynamic and surface conductances. An LST-driven water stress index is incorporated into STIC in the aerodynamic equations of  $H$  and  $\lambda E$  and a modified complementary relationship advection-aridity hypothesis (Mallick et al., 2015). The latest version of STIC combines the Shuttleworth-Wallace sparse canopy formulation model with the PM big-leaf model to calculate the vapour pressure at the source/sink height (Hu et al., 2023; Mallick et al., 2016, 2018, 2022).

## 2.2. Commonly used approaches for temporal upscaling of instantaneous ET

Various approaches have been proposed for retrieving daily ET from instantaneous satellite ET estimates (Table 1). These methods are generally categorized as either radiation-based or evaporative fraction-based. The EF method explicitly assumes the relative conservation of EF (defined as the ratio of latent heat flux to surface available energy) during the daytime. Once the daily integrated net available energy and the instantaneous EF at the satellite overpass are derived, the  $\text{ET}_d$  can be derived using the principle of diurnal conservation of EF. Gentine et al. (2007) reported that the degree to which the daytime EF is self-conservative depends upon the evaporation regime (water- or energy-limited) and the fractional vegetation cover. Furthermore, it was found that the daytime conservation of the EF curve occurs primarily under conditions of high relative humidity and solar radiation on clear-

sky days. The EF shows parabolic and convex patterns during the day at lower levels of incoming solar radiation (Gentine et al., 2011).

The concept of  $EF_r$  is similar to the definition of the crop coefficient that is widely used in agricultural water resources management. The ratio of the actual instantaneous ET to  $ET_d$  can be represented by the ratio of the corresponding reference instantaneous ET to  $ET_d$ , where the reference ET is the evapotranspiration from a reference surface that is not short of water and has specific characteristics. It was reported that the conservation of  $EF_r$  in a diurnal cycle could provide better estimates of the daily ET under the advective conditions that usually occur in the afternoon (Allen et al., 2007).

The  $R_g$  method relates the ratio of instantaneous to daily ET to variations of the diurnal global solar radiation considering the surface net radiation is the primary energy drivers of surface water and energy transfer on the land surface. Different methods have been developed to estimate the surface solar radiation, including the sinusoidal variation and machine learning approaches (Jackson et al., 1983; Wandera et al., 2017). There is a clear need for a simple yet robust hybrid method that integrates these factors to enable accurate and operational daily ET retrieval.

Although the aforementioned three methods have been widely used, a major challenge is to estimate the daily integrated variables (e.g., daily surface available energy, daily surface solar radiation). To overcome the challenge of estimating the daily integrated variables, Ryu et al. (2012) adopted the ratio of instantaneous to daily extraterrestrial solar radiation (i.e., solar radiation at the top of the Earth's atmosphere,  $R_p$ ) to upscale the remotely sensed ET to daily and eight-day averaged values. It was found that this ratio was a robust scaling factor based on the eddy covariance measurements from 34 instrumented towers in North America and Europe. However, it was also revealed that the  $R_p$  method failed to capture the effects of horizontal advection and atmospheric environment factors (e.g., wind speed, vapour pressure deficit) on the variations of the diurnal extraterrestrial solar radiation in the daily ET estimation.

**Table 1.** Summary of approaches used for temporal integration of instantaneous ET ( $ET_t$ ) to daily ET ( $ET_d$ ).

Name	Formula	Assumption	Limitations
EF (Brutsaert & Sugita, 1992)	$\frac{ET_d}{ET_t} \cong \frac{(R_N - G)_d}{(R_N - G)_t}$	Self-preservation of EF during the course of the day.	EF exhibits diurnal variability in semi-arid and humid climate and assumption of diurnal conservation of EF is only valid in arid ecosystems. Prone to error in areas where $ET_d$ is driven equally by radiation and soil moisture variability
EF <sub>r</sub> (Allen et al., 2007)	$\frac{ET_d}{ET_t} \cong \frac{ET_{d,r}}{ET_{t,r}}$	Constant ratio of actual ET to reference grass/alfalfa ET in a diurnal cycle	Requirement for detailed atmospheric variables, e.g., air temperature, relative humidity, and wind speed at half-hourly or hourly time scales
R <sub>g</sub> (Wandera et al., 2017)	$\frac{ET_d}{ET_t} \cong \frac{Rg_d}{Rg_t}$	$ET_d$ scales with daily surface	Only applicable for late morning to noontime acquisition times and in radiation-controlled ecosystems
R <sub>p</sub> (Ryu et al., 2012)	$\frac{ET_d}{ET_t} \cong \frac{Rp_d}{Rp_t}$	$ET_d$ scales with extra-terrestrial shortwave radiation	Only applicable for late morning to noontime acquisition times and in radiation-controlled ecosystems

In addition to the limitations outlined in Table 1 for current ET temporal upscaling approaches, the varying overpass time of the ECOSTRESS observations further challenges the usability of these methods, given the asynchronous orbit of the International Space Station. Upscaling instantaneous ECOSTRESS ET estimates at different times of the day to a daily scale requires explicit consideration of the diurnal variations of the constraining factors across different terrestrial ecosystems.

### 3. Look up table-based extraterrestrial radiation method

To facilitate the temporal integration of instantaneous ET estimates obtained at any time of the day into daily total ET, a robust hybrid LUT method has been developed. This method builds upon the foundational extraterrestrial solar radiation approach, enhancing it by incorporating a comprehensive set of variables, including longwave radiation, air temperature, atmospheric humidity, and solar radiation.

By integrating these variables, the method effectively captures the interactions between atmospheric conditions and land surface properties, providing a more nuanced understanding of ET dynamics. This approach ensures that the diurnal variability of ET is accurately represented, regardless of the time of satellite observation, enabling more reliable daily ET estimates across diverse ecosystems and climatic conditions.

The LUT is stratified by ecosystem type and satellite overpass time, ensuring its adaptability to diverse environmental conditions. The development follows a two-step process:

**Step-1: Calibration:** The LUT is first calibrated using data from the AmeriFlux sites, representing six different ecosystems—forest, grassland, cropland, shrubland, wetland, and savanna—across the contiguous United States. This step establishes baseline scaling factors tailored to each ecosystem type and the corresponding satellite overpass times.

**Step-2: Evaluation:** The calibrated LUT is then applied to ECOSTRESS ET estimates and rigorously evaluated using data from ICOS and EFDC sites across Europe. This ensures the method's robustness and applicability across varying geographical and climatic contexts. To maintain accuracy, the temporal range for satellite overpass time is restricted to the period between 8 am and 4 pm, where solar radiation and other diurnal factors are most stable for calibration and evaluation process.

The general form of the ET temporal upscaling method is as follows

$$ET_d = f_{LW} f_{RN} f_{TA} \frac{Rp_d}{Rp_t} ET_t \quad (3.1)$$

where  $ET_d$  and  $ET_t$  are the daily and instantaneous ET, respectively,  $f_{LW}$ ,  $f_{RN}$ , and  $f_{TA}$  are the factors related to longwave radiation, net radiation, and air temperature, respectively,  $R_{p_d}$  and  $R_{p_t}$  are the daily and instantaneous extra-terrestrial shortwave radiations, respectively, which can be calculated easily using astronomical equations. More specifically, the three scaling factors are expressed as follows

$$f_{LW} = \frac{L_{in}}{L_{out}} \quad (3.2)$$

$$f_{RN} = \frac{R_N}{R_g - R_r + L_{in}} \quad (3.3)$$

$$f_{TA} = \frac{T_a}{T_{a,max}} \quad (3.4)$$

where  $L_{in}$  and  $L_{out}$  are the atmospheric downwelling longwave radiation and surface upwelling longwave radiation, respectively.  $R_N$  is the surface net radiation,  $R_g$  is the surface solar radiation,  $R_r$  is the surface reflected solar radiation.  $T_a$  is the air temperature,  $T_{a,max}$  is the maximum air temperature during the course of the day. All the variables (except for  $T_{a,max}$ ) are instantaneous at the satellite overpass time.

### 3.1. Selection of the constraining factors

The three constraining factors in Eq. 3.1 encapsulate distinct aspects of atmospheric and land surface conditions:

**$f_{LW}$** : This factor reflects the humidity and thermal states of both the atmosphere and land surface, effectively capturing the combined influence of atmospheric transmissivity and surface water availability. It provides critical insight into how these two elements interact to regulate energy fluxes.

**$f_{RN}$** : This factor conveys information about solar radiation, compounded with the surface thermal condition. By integrating these components,  $f_{RN}$  highlights the role of incoming solar energy and its interaction with the surface in driving ET dynamics.

$f_{TA}$ : Acting as a proxy for midday LST-induced stress, this factor represents the impact of elevated land surface temperatures during peak solar hours, which can significantly influence the energy balance and evapotranspiration processes.

These factors collectively provide a comprehensive representation of the interplay between atmospheric conditions and land surface properties, enabling a nuanced understanding of ET variability.

Only one of the three scaling factors from the three is applied to constrain the temporal integration in each scenario, depending on the prevailing radiation and water stress conditions.  $f_{LW}$  is typically used when there is a significant difference between the surface solar radiation and extraterrestrial solar radiation. In such cases,  $f_{LW}$  accounts for atmospheric transmissivity, effectively capturing the impact of varying atmospheric conditions on energy fluxes. The factor  $f_{RN}$  is employed when solar radiation is the primary limiting factor in the SEB process. It is mostly applicable during early morning and late afternoon hours in energy-constrained ecosystems.  $f_{TA}$  is used when solar radiation is abundant, particularly around midday. It is especially relevant in water-constrained ecosystems, where land surface temperature-induced stress becomes a critical factor in regulating ET. It is also worth noting that the original  $R_p$  method tends to perform better without the inclusion of any constraining factors, depending on the specific surface and atmospheric conditions. This highlights the importance of carefully selecting the appropriate scaling factor to optimize temporal integration for varying scenarios.

To select the proper constraining factor for various overpass times and ecosystems, the original  $R_p$  method is used as the basis. The newly developed method is compared with the  $R_p$  method. The potential constraining factors are selected for each hour and the  $ET_d$  estimates are compared with the ones obtained using the  $R_p$  method. The best performing method is selected for each hour in the different ecosystems. RMSE and bias are adopted as the metrics to measure the accuracy of the  $ET_d$  estimates.

### 3.2. Calibration of the LUT

Eddy covariance measurements at the selected AmeriFlux sites are used to calibrate the LUT. The sites used for different ecosystems are listed in Table 2. Six different ecosystems are encompassed, which are the major types. The samples used for the calibration are over 1000 for each site, which indicates a good representation of various conditions.

**Table 2.** AmeriFlux sites used for the calibration of LUT in six different ecosystems. Due to the various data available times, the measurements at different sites are collected during different years between 2000 and 2023.

Land cover	Site	Latitude	Longitude	Aridity Index	Sample Number
Forest	US-NR1	40.0329	-105.5464	0.4307	3171
	US-Me2	44.4526	-121.5589	0.7376	4848
	US-Me6	44.3233	-121.6078	0.4057	4541
Grassland	US-Wkg	31.7365	-109.9419	0.1682	6249
	US-SRG	31.7894	-110.8277	0.2232	6561
	US-Ro4	44.6781	-93.0723	0.7088	3377
	US-xAE	35.4141	-99.0588	0.3546	3549
	US-xCP	40.8255	-104.7456	0.2126	3533
	US-xKA	39.1104	-96.6129	0.5696	2701
	US-xKZ	39.1008	-96.5631	0.5769	4044
	US-xDC	47.1617	-99.1066	0.3792	2926
	US-xCL	33.4012	-97.57	0.4713	2494
	US-xNG	46.7697	-100.9154	0.3367	3396
	Cropland	US-Bi1	38.0992	-121.4993	0.222
US-Bi2		38.1091	-121.5351	0.221	2896
US-Ro5		44.691	-93.0576	0.7068	1887
US-Ro6		44.6946	-93.0578	0.7094	1950
US-ARM		36.6058	-97.4888	0.4922	2691
US-Mo1		39.2298	-92.1167	0.751	2718
US-xSL		40.4619	-103.0293	0.2474	3003
Shrubland	US-Whs	31.7438	-110.0522	0.1499	5324
	US-Rws	43.1675	-116.7132	0.2082	4202
	US-Rms	43.0645	-116.7486	0.3529	2134
	US-Rwf	43.1207	-116.7231	0.3049	2116
	US-xJR	32.5907	-106.8425	0.116	1533
	US-xNQ	40.1776	-112.4524	0.1652	2279
	US-xSR	31.9107	-110.8355	0.1549	3758
	US-xMB	38.2483	-109.3883	0.1746	1057
	US-xHE	63.8757	-149.2133	0.7021	2091
Wetland	US-NC4	35.7879	-75.9038	0.9588	2254
Savanna	US-Ton	38.4309	-120.966	0.3442	2128
	US-xSJ	37.1088	-119.7323	0.2686	2604

Eq. 3.1 is calibrated independently for each ecosystem type based on eddy covariance measurements. To account for the low magnitude of solar radiation during early morning and late afternoon hours, the calibration period is constrained between 8 am and 4 pm. Hourly

scaling factors are calibrated based on the ecosystem type. The optimal scaling factors are selected by comparing the results of the calibration against commonly used upscaling methods listed in Table 1, which serve as references. Based on this selection process, the LUT for ET<sub>d</sub> integration is constructed as shown in Table 3.

In EEH2, the meteorological data required for ET temporal upscaling, including air temperature, atmospheric humidity, and surface solar radiation are sourced from the ERA5 reanalysis dataset. The maximum air temperature is derived from the hourly air temperature in ERA5. The atmospheric longwave radiation is calculated based on the atmospheric humidity and temperature conditions, while the surface upwelling longwave radiation is calculated based on the ECOSTRESS surface temperature and emissivity estimates retrieved using the temperature and emissivity separation algorithm (refer to EEH-LST-ATBD for more detail). The surface reflected solar radiation is calculated based on the ERA5 surface solar radiation and the surface albedo data from the Copernicus Global Land Service (CGLS, <https://land.copernicus.eu/en>). The net radiation is calculated by combining the four components of surface radiation budget as mentioned before. The detail of data use is listed in Table 4.

**Table 3.** LUT for ET temporal upscaling calibrated using the ground measurements at the AmeriFlux eddy covariance sites in different ecosystems. RN, TA, and LW indicate the adopted constraining factors, i.e.,  $f_{RN}$ ,  $f_{TA}$ , and  $f_{LW}$ . For each time slot, one dominant constraining factor is used in Eq. 3.1.

Ecosystem	8	9	10	11	12	13	14	15	16
Forest	$f_{RN}$	$f_{RN}$	$f_{RN}$	$f_{RN}$	$f_{RN}$	-	-	-	-
Grassland	-	-	-	-	-	-	-	-	-
Cropland	-	-	-	$f_{TA}$	$f_{TA}$	$f_{TA}$	$f_{TA}$	$f_{TA}$	$f_{TA}$
Shrubland	-	-	-	-	-	-	-	-	-
Wetland	$f_{LW}$	$f_{LW}$	$f_{LW}$	$f_{TA}$	$f_{TA}$	$f_{TA}$	$f_{TA}$	$f_{LW}$	$f_{LW}$
Savanna	$f_{RN}$	$f_{LW}$	$f_{LW}$	$f_{TA}$	$f_{TA}$	$f_{TA}$	$f_{TA}$	$f_{TA}$	$f_{TA}$

**Table 4.** Input parameters for daily ET integration from different sources, including ECOSTRESS LST and emissivity products, ECOSTRESS instantaneous ET product, CGLS surface parameters, and

ERA5 reanalysis meteorological data. The CGLS and ERA5 are spatially (bilinearly) and temporally (linearly) interpolated to match the ECOSTRESS LST data.

Data	Purpose	Source	Spatial	Temporal
LST	Surface upwelling longwave radiation	ECOSTRESS	~70 m	Daily
Emissivity	Surface upwelling longwave radiation	ECOSTRESS	~70 m	Daily
ET	Instantaneous ET	ECOSTRESS	~70 m	Daily
Albedo	Surface reflected shortwave radiation	CGLS	1 km	10-day
Air temperature	Constraining factor	ERA5	0.25 deg	Hourly
Atmospheric humidity	Surface downwelling longwave radiation	ERA5	0.25 deg	Hourly
Surface solar radiation	Net radiation	ERA5	0.25 deg	Hourly
Maximum air temperature	Constraining factor	ERA5	0.25 deg	Hourly

### 3.3. Evaluation of the LUT-based extraterrestrial radiation method

The compiled LUT is evaluated using the selected independent sites from EFDC and ICOS. A total of 19 sites in six different ecosystems are selected in the evaluation to cover all the scenarios. The detailed sites are listed in Table 5. The evaluation results from the selected sites across different ecosystems are shown in Figs. 1 – 4. In total, approximately 100 samples are used in the evaluation of the proposed new method, based on the clear-sky ECOSTRESS extracts between 2018 and 2021 and availability of the measured latent heat fluxes at the eddy covariance sites during the course of the day.

**Table 5.** List of the selected eddy covariance flux sites. The biomes are according to the IGBP classification, and climate is according to the Köppen climate type. Biomes covered in this study include deciduous broadleaf forest (DBF), evergreen needleleaf forest (ENF), mixed forest (MF), savanna (SAV), cropland (CRO), grassland (GRA), shrubland (SHR) and wetland (WET). Climate types include humid subtropical (Cfa), temperate oceanic (Cfb), hot-summer Mediterranean (Csa), hot-summer humid continental (Dfa), warm-summer humid continental (Dfb), and subarctic (Dfc). Mean annual

precipitation (MAP) and aridity index (AI) indicate the aridity level at the sites. AI is calculated as the ratio between precipitation and potential ET for 30 years and indicates the local climatology.

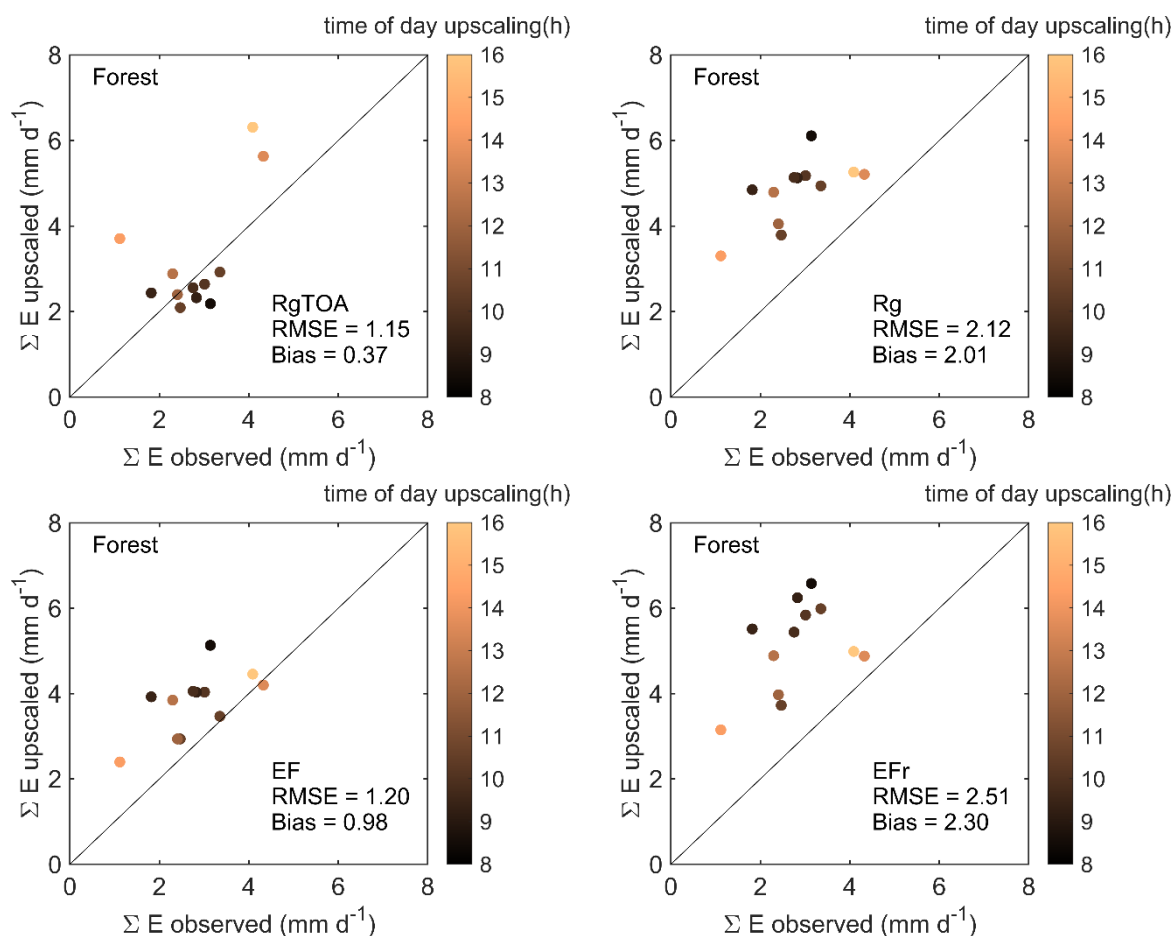
Site ID	Biome	Climate	Latitude (°)	Longitude (°)	MAP (mm)	AI	Source
BE-Lcr	DBF	Cfb	51.11	3.85	861	0.93	ICOS
BE-Lon	CRO	Cfb	50.55	4.75	743	0.97	ICOS
BE-Maa	SHR	Cfb	50.98	5.63	839	0.93	ICOS
BE-Vie	MF	Cfb	50.31	6.00	1062	1.37	EFDC
CZ-Wet	WET	Dfa	49.03	14.77	604	0.74	EFDC
DE-Geb	CRO	Cfb	51.10	10.92	470	0.58	EFDC
DE-Gri	GRA	Dfb	50.95	13.51	872	0.91	ICOS
DE-Kli	CRO	Dfb	50.89	13.52	842	1.00	EFDC
DE-Rur	GRA	Cfb	50.62	6.30	1033	1.38	EFDC
DE-RuS	CRO	Dfb	50.87	6.45	698	0.82	ICOS
ES-LM1	SAV	Csa	39.94	-5.78	700	0.30	EFDC
ES-Abr	SAV	Csa	38.70	-6.79	400	0.32	EFDC
FR-Aur	CRO	Cfb	43.55	1.11	669	0.74	ICOS
FR-Bil	ENF	Cfb	44.49	-0.96	960	0.89	ICOS
FR-Hes	DBF	Cfb	48.67	7.07	820	0.89	EFDC
FR-LGt	WET	Cfb	47.32	2.28	700	0.73	ICOS
FR-Mej	GRA	Cfb	48.12	-1.80	722	0.79	ICOS
IT-Lsn	SHR	Cfa	45.74	12.75	1100	0.91	ICOS
IT-Tor	GRA	Dfc	45.84	7.58	945	1.42	ICOS

The developed LUT method demonstrates a comparable RMSE to the widely used EF method in forests and croplands but with much simplified input parameters, where water stress is not a significant constraint. In contrast, the RMSEs of the other two methods ( $EF_r$  and  $R_g$ ) are notably higher. The challenge in retrieving accurate input parameters for these two methods could further deteriorate their performances. Additionally, the biases of the developed LUT method in less water stressed ecosystems are close to 0, which are notably lower than that of the EF method. As compared to the other two methods, the overestimation in the estimated  $ET_d$  is well corrected.

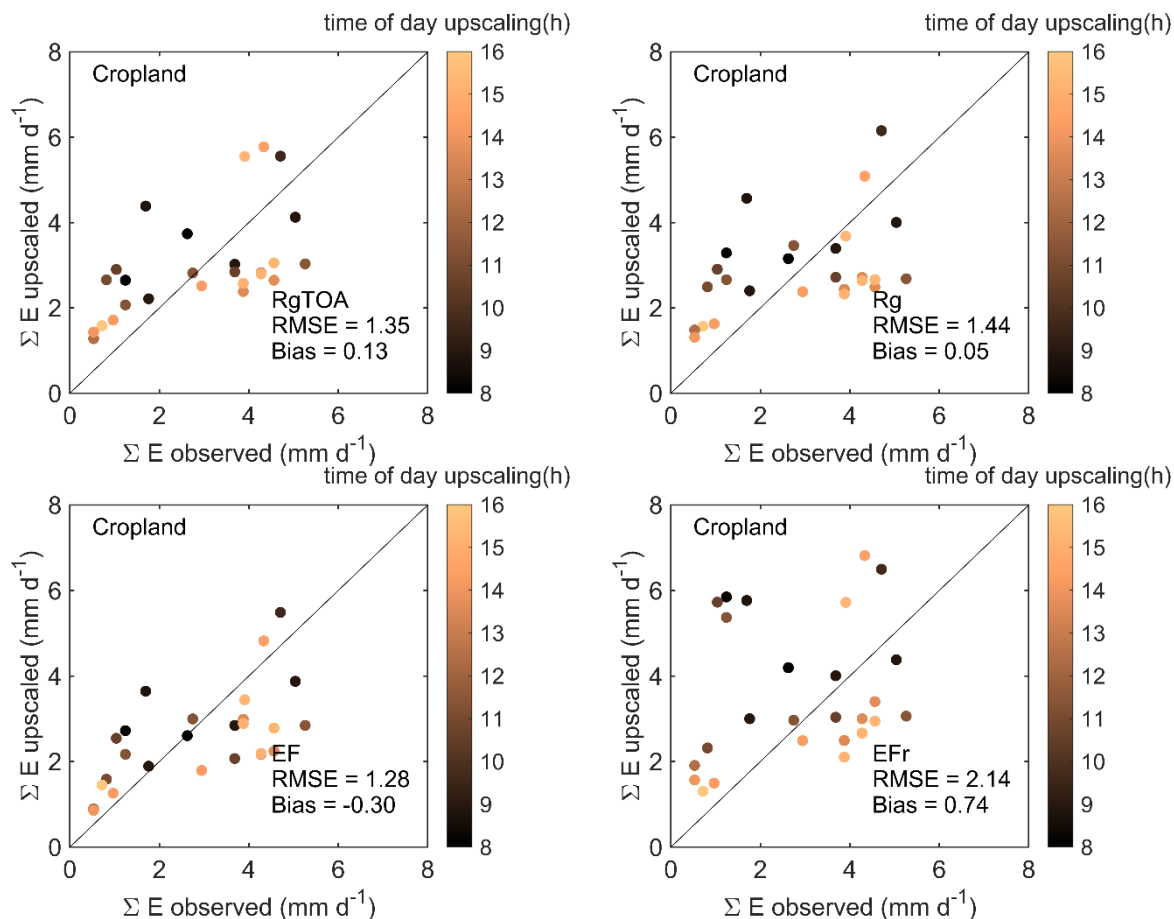
A key advantage of the LUT method is observed in savanna ecosystems (Fig. 4), which are severely constrained by water availability. For these water-limited regions, the developed LUT method achieves an RMSE below 1 mm/day, showcasing its robustness and reliability. The EF method shows an RMSE above 1 mm/day although the bias is close to 0. Similar to the worse performances in the radiation constrained ecosystems, the other two methods have

RMSEs close to 2 mm/day, which shows the large uncertainties of these two temporal integration methods.

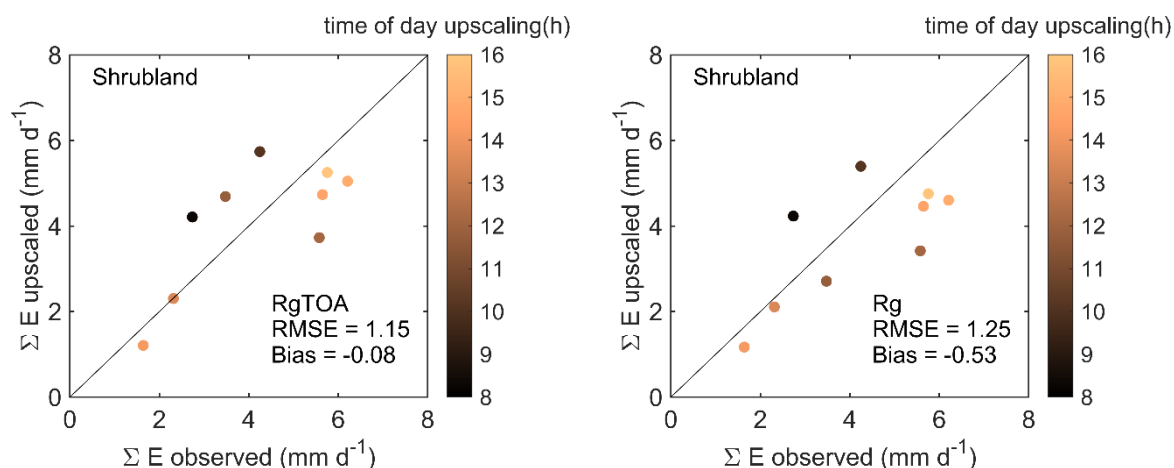
Overall, the newly developed method achieves satisfying performance in various ecosystems compared to the other three widely used upscaling methods. Moreover, the input parameters are easily accessible without severe uncertainties. This is a significant advantage over the other methods that rely on daily integrated radiation or reference ET at the satellite scale.



**Fig. 1.** Evaluation of the LUT-based extraterrestrial solar radiation method at the forest sites, along with the commonly used ET temporal upscaling methods. Rg<sub>TOA</sub>, R<sub>g</sub>, EF, and EF<sub>r</sub> represent the developed LUT method, surface solar radiation method, evaporative fraction method, and the reference evaporative fraction method.



**Fig. 2.** Evaluation of the LUT-based extraterrestrial solar radiation method at the cropland sites, along with the commonly used ET temporal upscaling methods. Rg<sub>TOA</sub>, Rg, EF, and EFr represent the developed LUT method, surface solar radiation method, evaporative fraction method, and the reference evaporative fraction method.



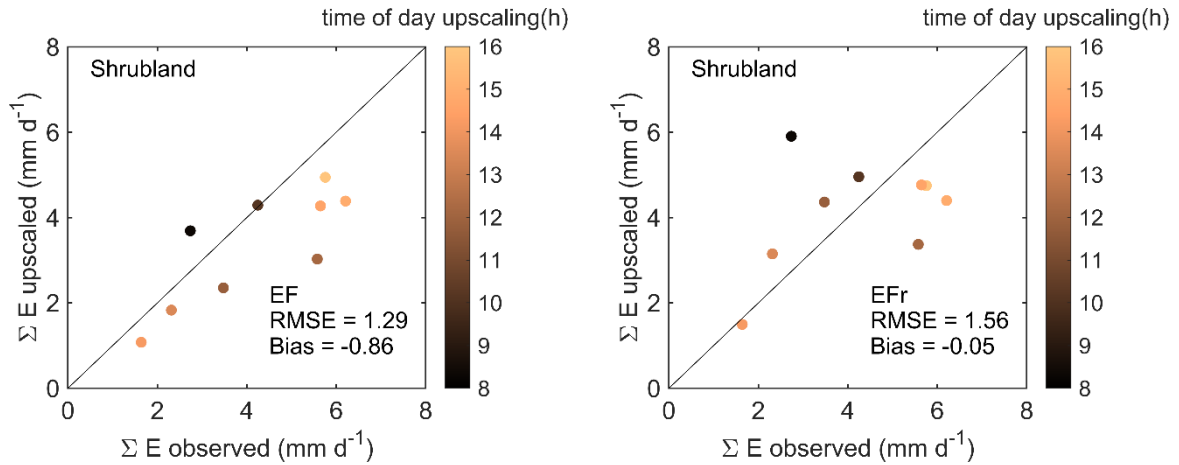


**Fig. 3.** Evaluation of the LUT-based extraterrestrial solar radiation method at the shrubland sites, along with the commonly used ET temporal upscaling methods.  $Rg_{TOA}$ ,  $R_g$ , EF, and  $EF_r$  represent the developed LUT method, surface solar radiation method, evaporative fraction method, and the reference evaporative fraction method.

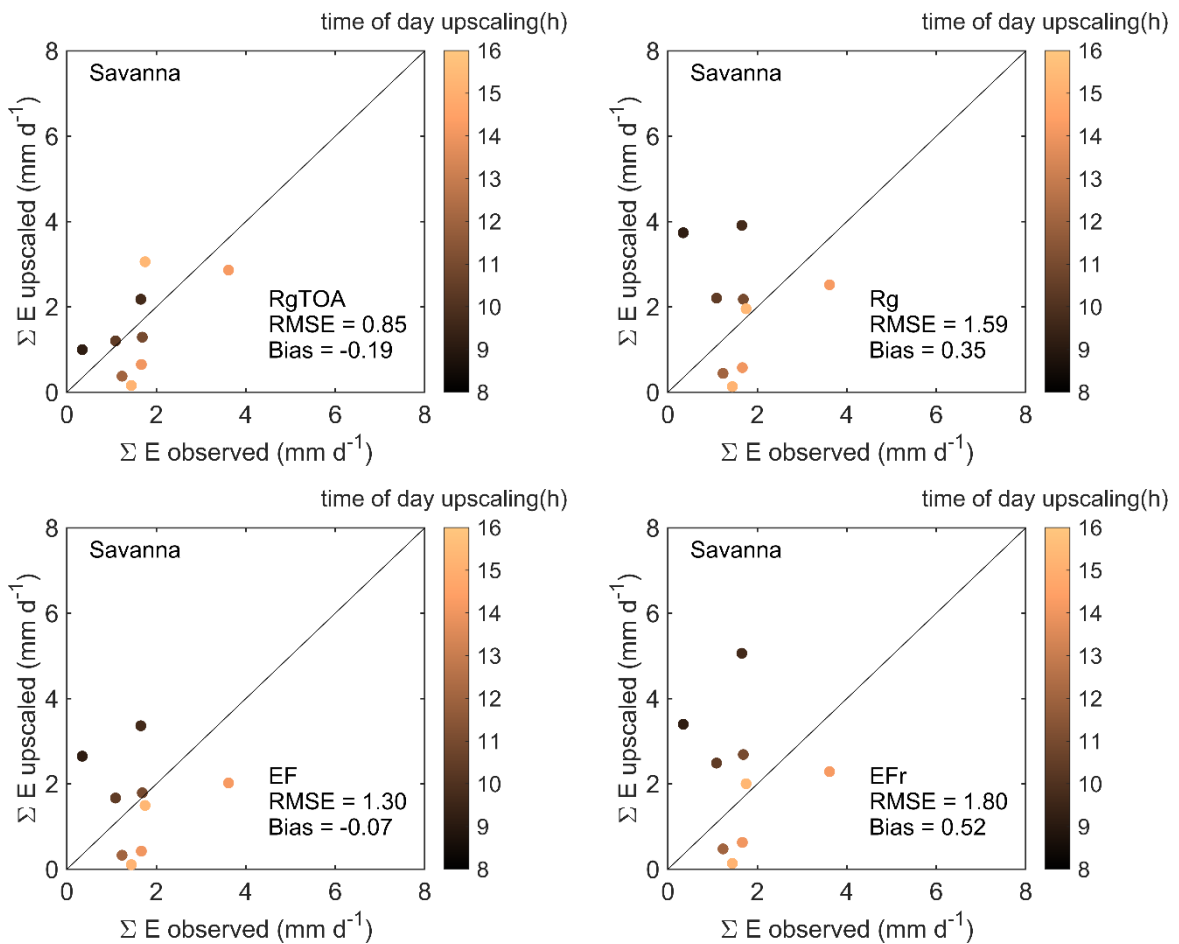


**Fig. 4.** Evaluation of the LUT-based extraterrestrial solar radiation method at the savanna sites, along with the commonly used ET temporal upscaling methods.  $Rg_{TOA}$ ,  $R_g$ , EF, and  $EF_r$  represent the

developed LUT method, surface solar radiation method, evaporative fraction method, and the reference evaporative fraction method.

Based on the evaluation results, it is evident that the developed LUT method has a satisfactory performance in daily ET estimation, especially in comparison to the other commonly used methods. It is worth mentioning that the newly developed ET integration method is not constrained by the SEB model used for ET retrieval and can be extended to any other instantaneous ET estimates. Considering the easily available input parameters for the upscaling, the developed LUT method has promise for retrieving daily ET from the future high-resolution thermal missions, including TRISHNA, SBG, and LSTM.

## **Acknowledgement**

The research was carried out at the Luxembourg Institute of Science and Technology, under a contract with the European Space Agency.

## Reference

- Allen, R. G., Tasumi, M., & Trezza, R. (2007). Satellite-based energy balance for mapping evapotranspiration with internalized calibration (METRIC)—Model. *Journal of Irrigation and Drainage Engineering*, 133(4), 380–394.
- Brutsaert, W., & Sugita, M. (1992). Application of self-preservation in the diurnal evolution of the surface energy budget to determine daily evaporation. *Journal of Geophysical Research: Atmospheres*, 97(D17), 18377–18382.
- Dai, A. (2013). Increasing drought under global warming in observations and models. *Nature Climate Change*, 3(1), 52–58.
- Galleguillos, M., Jacob, F., Prévot, L., Lagacherie, P., & Liang, S. (2010). Mapping daily evapotranspiration over a Mediterranean vineyard watershed. *IEEE Geoscience and Remote Sensing Letters*, 8(1), 168–172.
- Gentine, P., Entekhabi, D., Chehbouni, A., Boulet, G., & Duchemin, B. (2007). Analysis of evaporative fraction diurnal behaviour. *Agricultural and Forest Meteorology*, 143(1–2), 13–29.
- Gentine, P., Entekhabi, D., & Polcher, J. (2011). The diurnal behavior of evaporative fraction in the soil–vegetation–atmospheric boundary layer continuum. *Journal of Hydrometeorology*, 12(6), 1530–1546.
- Hu, T., Mallick, K., Hitzelberger, P., Didry, Y., Boulet, G., Szantoi, Z., Koetz, B., Alonso, I., Pascolini-Campbell, M., & Halverson, G. (2023). Evaluating European ECOSTRESS hub evapotranspiration products across a range of soil-atmospheric aridity and biomes over Europe. *Water Resources Research*, 59(8), e2022WR034132.
- Jackson, R. D., Hatfield, J. L., Reginato, R. J., Idso, S. B., & Pinter Jr, P. J. (1983). Estimation of daily evapotranspiration from one time-of-day measurements. *Agricultural Water Management*, 7(1–3), 351–362.
- Jasechko, S., Sharp, Z. D., Gibson, J. J., Birks, S. J., Yi, Y., & Fawcett, P. J. (2013). Terrestrial water fluxes dominated by transpiration. *Nature*, 496(7445), 347–350.
- Mallick, K., Baldocchi, D., Jarvis, A., Hu, T., Trebs, I., Sulis, M., Bhattarai, N., Bossung, C., Eid, Y., & Cleverly, J. (2022). Insights into the aerodynamic versus radiometric surface temperature debate in thermal-based evaporation modeling. *Geophysical Research Letters*, 49(15), e2021GL097568.
- Mallick, K., Boegh, E., Trebs, I., Alfieri, J. G., Kustas, W. P., Prueger, J. H., Niyogi, D., Das, N., Drewry, D. T., & Hoffmann, L. (2015). Reintroducing radiometric surface temperature into the P enman-M onteith formulation. *Water Resources Research*, 51(8), 6214–6243.
- Mallick, K., Jarvis, A. J., Boegh, E., Fisher, J. B., Drewry, D. T., Tu, K. P., Hook, S. J., Hulley, G., Ardö, J., & Beringer, J. (2014). A Surface Temperature Initiated Closure (STIC) for surface energy balance fluxes. *Remote Sensing of Environment*, 141, 243–261.
- Mallick, K., Toivonen, E., Trebs, I., Boegh, E., Cleverly, J., Eamus, D., Koivusalo, H., Drewry, D., Arndt, S. K., & Griebel, A. (2018). Bridging thermal infrared sensing and physically-based evapotranspiration modeling: from theoretical implementation to validation across an aridity gradient in Australian ecosystems. *Water Resources Research*, 54(5), 3409–3435.

Mallick, K., Trebs, I., Boegh, E., Giustarini, L., Schlerf, M., Drewry, D. T., Hoffmann, L., Von Randow, C., Kruijt, B., & Araùjo, A. (2016). Canopy-scale biophysical controls of transpiration and evaporation in the Amazon Basin. *Hydrology and Earth System Sciences*, 20(10), 4237–4264.

Ryu, Y., Baldocchi, D. D., Black, T. A., Detto, M., Law, B. E., Leuning, R., Miyata, A., Reichstein, M., Vargas, R., & Ammann, C. (2012). On the temporal upscaling of evapotranspiration from instantaneous remote sensing measurements to 8-day mean daily-sums. *Agricultural and Forest Meteorology*, 152, 212–222.

Tang, R., Li, Z.-L., & Sun, X. (2013). Temporal upscaling of instantaneous evapotranspiration: An intercomparison of four methods using eddy covariance measurements and MODIS data. *Remote Sensing of Environment*, 138, 102–118.

Wandera, L., Mallick, K., Kiely, G., Roupsard, O., Peichl, M., & Magliulo, V. (2017). Upscaling instantaneous to daily evapotranspiration using modelled daily shortwave radiation for remote sensing applications: an artificial neural network approach. *Hydrology and Earth System Sciences*, 21(1), 197–215.